Fizika Nizkikh Temperatur, 1996, v. 22, No 2, p. 189–193

Ions in superfluid helium: measurement of the roton limited mobility

H. Günther, M. Foerste, G. zu Putlitz, and Th. Schumacher

Physikalisches Institut der Universität Heidelberg, Philosophenweg 12, D-69120 Heidelberg, Deutschland
E-mail:guenther@physi.uni-heidelberg.de

Different ions are used as microscopic probes for superfluid helium at temperatures ranging from 1.3 to 2.2 K. The ionic mobilities may provide new insight into the so far not well understood microscopic ion–roton scattering process. An ion source, which allows implantation of a great variety of impurity ions into liquid helium, is presented. Low-field velocities of Na^+, Ag^+ and Au^+ ions are reported as a function of the electrical drift field and the temperature. Moreover, a temporal series of images taken by an intensifying CCD camera is presented, showing a cloud of moving Ba^+ ions.

1. Introduction

Mobility studies of electrons and He^+ ions in liquid helium have proven to be an appropriate tool to investigate both the quantum liquid itself and the defect structures of foreign ions. According to the two-fluid model [1], He II is capable of supporting two kinds of motion at the same time: the nonviscous superfluid flow and the normal-fluid flow. The total density ρ is described as the sum of the densities of normal-fluid ρ_n and superfluid ρ_s components.

However, the two-fluid model and other theoretical approaches are not able to explain the mobility of ions in He II. There does not still exist any satisfactory theory concerning the scattering of thermal excitations, namely the rotons. For this reason it seems promising to study the quantum liquid from a microscopic point of view. Researchers have successfully used atoms and ions as microscopic probes for He II: mobility measurements (for references see below) as well as optical experiments [2–4] have deepened the knowledge of both the quantum fluid itself and its interaction with these implanted atoms and ions.

Inside the liquid the probe particles build so called *bubbles* and *snowballs* depending on their charge, polarizability, and valence electron configuration [5,6]. The electron and, most likely, the positive alkali earth ions make up cavities in liquid helium with a radius of 7 to 18 Å, whereas the positive helium ion and the alkali ions are assumed to form solid structures with a radius of 7 to 10 Å. The effective mass of the electron bubble was found to be about $240 m_{He}$, and that of the He^+ snowball $44 m_{He}$ at saturated vapor pressure [7].

The thermal excitations (phonons and rotons) behave like a gas of quasi-particles in the background fluid. They constitute the normal fluid fraction and carry all the entropy of He II. In the *kinetic regime* — in the temperature range $0.8\ K < T < 1.7\ K$ — predominantly rotons determine the thermodynamic properties of He II. Their density n_r can be calculated from the energy-momentum dispersion relation for rotons: $\varepsilon = \Delta + (p - p_0)^2/2\mu_r$. The energy gap $\Delta/k_B = 8.65$ K, the roton mass parameter $\mu_r = 0.16 m_{He}$ and $p_0/\hbar = 19.1\ nm^{-1}$ were determined from neutron scattering data [8].

In low electric fields E the drift velocity $\langle v_d \rangle$ of ions in liquid helium is proportional to E and thus the mobility $\mu(T) = \langle v_d \rangle / E$ is constant for a given temperature. The low-field mobility in the kinetic regime was found [9] to be proportional to the inverse roton density: $\mu^{-1} \propto \exp(-\Delta/k_B T)$. The condition for low electric fields is that the electric energy of the ion gained between two collisions with rotons is well below the thermal energy of the ions: $Ee\lambda_{ion} \ll 3/2\, k_B T$. Here λ_{ion} denotes the mean free path of the ions.

In high electric fields, the ions can reach the *Landau critical velocity* v_L. Particles moving at $v_L = 58$ m/s have sufficient energy and momentum to create elementary excitations (namely, the rotons). The mean drift velocity is no longer proportional to the electric field. The Landau critical velocity was carefully studied by McClintock et al. [10] who found an evidence for *roton–pair creation* to be the significant process limiting $\langle v_d \rangle$ to v_L. However, roton emission can only be observed in pressurized liquid helium where the formation of the so-called charged ion-vortex states is suppressed. In the case of low pressure the limiting mechanism for $\langle v_d \rangle$ is the creation of vortex rings rather than roton emission: with increasing electric drift field in this region, $\langle v_d \rangle$ drops to very low values [12].

Glaberson and Johnson [11] extended the mobility measurements for the first time to foreign ions. They examined the drift properties of the alkali ions K^+, Rb^+, Cs^+ and of the alkali earth ions Ca^+, Sr^+, Ba^+ in low and high electric fields. In low electric drift fields they found remarkably high mobilities of the alkali earth ions compared to the He^+ ion. The low-field mobilities of Ca^+, Sr^+, Ba^+ were found to increase with increasing atomic number. Two isotopes, ^{40}Ca and ^{48}Ca, are used to examine the mobility as a function of mass and temperature.

From mobility measurements in high electric fields — in this case the mobility is limited by vortex-bound ionic states — ionic radii were estimated. Applying a simplified approach of Reif and Meyer [9], the calculated mobilities are found to agree only qualitatively with the experimental data.

Several detailed approaches were made to develop an exact theory for the roton-limited mobility of ions in superfluid helium [9,12–14]. However, it is not possible for all impurity ions to explain the temperature dependence of the mobility. The crucial points are the lack of knowledge about the ion effective mass m_{ion} and the not well understood ion-roton scattering cross section σ_{ir}. The assumption of hard spheres for the rotons and ions and a momentum-independent σ_{ir} are not too good descriptions for the real scattering process.

To compare with more detailed theoretical approaches [13], additional mobility data are required. It seemed reasonable to perform further mobility studies with foreign ions in a more extended temperature and pressure ranges. As to the alkali and alkali earth ions, there are only assumptions about the real structure of the positive ion complex. Here mobility measurements may play an important role to characterize the kind and size of these impurities in liquid helium.

In this paper we present a method which allows a great variety of foreign ions to be implanted into He II and mobility studies to be performed in the temperature range of 1.3 to 2.2 K. The drift time of ions in electric field is measured in two different ways: a) by electrical signals of the ions and b) by optical signals due to the light emission of recombining ions. First results for Na^+, Ag^+ and Au^+ ions are reported here. Moreover, a spatially resolved pattern of drifting Ba^+ ions is demonstrated.

2. Experimental set-up

This Section will serve as an introduction to the experimental set-up and the method of mobility measurements of ions in liquid helium.

The experiments are carried out inside a ^4He bath cryostat. Two Roots pumps serve to cool down the liquid helium bath by reducing the vapor pressure. The maximum pumping rate at 1 mbar is about 600 $m^3 \cdot h^{-1}$ and can be controlled through several valves. At saturated vapor pressure a temperature range 1.3–4.2 K can be covered. The temperature is measured through the vapor pressure of helium and by a calibrated carbon resistor (Allan Bradley). The accuracy during one-day run is better than 1 mK.

A cube-shaped chamber is submerged in the liquid helium bath [3,15]. This chamber contains an ion source in the gas phase, a set-up for the implantation of ions into the liquid, a homogeneous electrical field for drift time measurements and an electrical detection system for the ions. A magnetic needle valve at the bottom of the cell ensures constant liquid helium level right between the ion source and the time of flight area.

The ions are implanted into liquid helium using two different methods. a) The probe material is evaporated in a small oven and subsequently ionized in a helium gas discharge [16]. This method is suitable for a continuous flow of ions, especially for metals with a low melting point. On the other hand, the ion production is restricted to temperatures below 1.5 K (equivalent to a vapor pressure of 10 mbar) because otherwise the helium gas discharge becomes unstable. b) The probe material is evaporated and ionized in the focus of a pulsed laser beam [17] (Fig. 1). A great variety of metals and even ionic crystals can be used as probes because of the high temperatures achieved in the laser focus. A nitrogen laser (1 to 3 mJ for 10 ns pulses) is focused onto the probe through a quartz lens having a focal length of 15 mm. The measurements presented in this contribution were carried out only with the laser sputtering method because of the

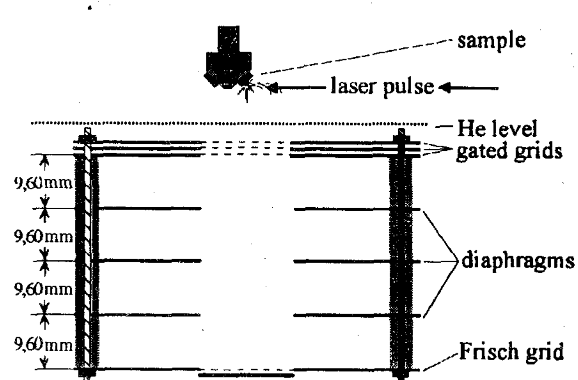

Fig. 1. Experimental chamber with ion production by laser sputtering and drift cell for mobility studies.

easier handling and the greater range of temperatures that can be covered (1.3 to 2.2 K).

The positive ions produced above the helium surface are drawn into the liquid by means of an electric field. Three electrically charged grids directly below the liquid level permit manipulation of the ion current (Fig. 1). The upper grid controls the electric field for ion implantation. The second and third grids serve as a gate for the ions. By applying an appropriate voltage to the second grid for a short period of time (1 to 10 ms), ions are allowed to drift towards the collector. Three diaphragms are used to guarantee a homogeneous drift field. Additionally there is a grid mounted directly above the collector. This so-called Frisch grid serves as an electric shield to protect the collector against induced image charges resulting from the approaching ion cloud.

Finally, the collector is connected to a sensitive current amplifier, able to detect typical ion currents of 100 pA to 10 nA. Through an opto-electronic transducer the amplified collector current is read out and registered as a function of time. Thus the drift time of different ionic species can be determined.

The measurements were taken at low drift fields where the mobility is constant. The applied voltage was 50 to 300 V at a drift distance of 4.160 cm (Fig. 1). Precisely manufactured copper spacers of 0.960 cm between each diaphragm and a stabilized power supply for the drift voltage ensures a homogeneous and reproducible electric field. Due to thermal effects the copper spacers contract by 0.3 % [18] during the cooling from room temperature to liquid helium temperature.

The ions were detected not only electrically at the collector as described above but optically as well using a photomultiplier and an image intensifying CCD camera. For this purpose a field emission tip was used. Electrons emerging from this tip move in the opposite direction relative to positive charged foreign ions. They approach each other and recombine to excited neutral atoms. During this process and the subsequent relaxation to a new equilibrium state an energy of about 1.8 eV is dissipated into the liquid for each recombining ion [3,19]. Usually the excited atoms emit light during their de-excitation. These photons were detected as a function of position, time and wavelength to determine the time-dependent distribution and the density of atoms in liquid helium.

3. Experimental results

In this paper the low-field velocities of Na^+, Ag^+ and Au^+ as a function of the drift field E and the temperature are presented. Moreover, results of optical mobility measurements on Ba^+ ions through the image intensifying CCD camera are shown. Further mobility studies are in progress [20] for light-mass alkali and alkali earth ions as well as transition metal ions to provide more data for the roton-ion scattering process.

In each time of flight spectrum of foreign ions drifting through liquid helium a great number of various peaks is detected. For Na^+ ions two large and at least three smaller peaks are observed (Fig. 2). By comparing these data with the mobility of He^+ ions, the peak 3 is assigned to Na^+ ions and peak 4 to He^+ ions. The process of ion production is such that He^+ ions are very likely to be present, in addition to the probe ions. The two very fast peaks 1 and 2 are assumed to be caused by impurities on the surface of the Na sample. The amplitudes of these peaks varied considerably when the focus of the sputtering laser (Fig. 1) was scanned over the surface of the Na sample. Peak 5

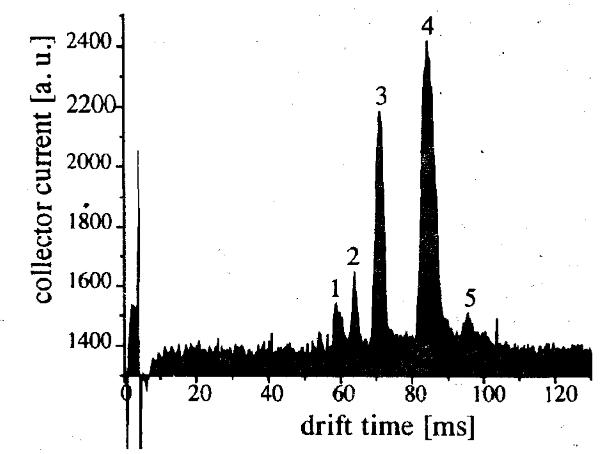

Fig. 2. Time of flight measurements on Na^+ and He^+ ions in liquid helium at $T = 1.42$ K and $E = 96\ V\cdot cm^{-1}$. Peaks 1 to 5 are due to different fast, positive charged ions or molecules produced during the sputtering process. See text for assignment of the signals.

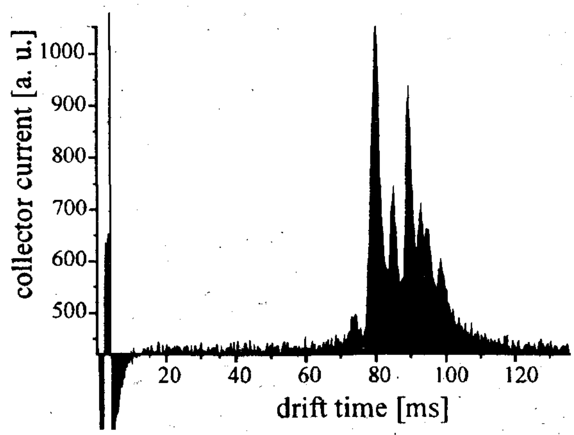

Fig. 3. Time of flight measurements on Ag^+ and He^+ ions in He II at $T = 1.39$ K and $E = 96\ V\cdot cm^{-1}$. The signals are due to different fast ions and molecular clusters. No complete assignment was possible. (See text.)

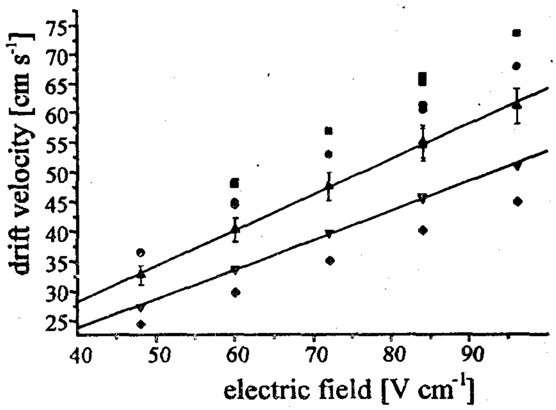

Fig. 4. The drift velocity of Na^+ ions as a function of the electric drift field at 1.42 K. The data for $E = 96\ V\cdot cm^{-1}$ correspond to the peak centers of Fig. 2: the peaks 1 to 5 are represented by squares, circles, triangles, upside-down triangles, and diamonds, respectively.

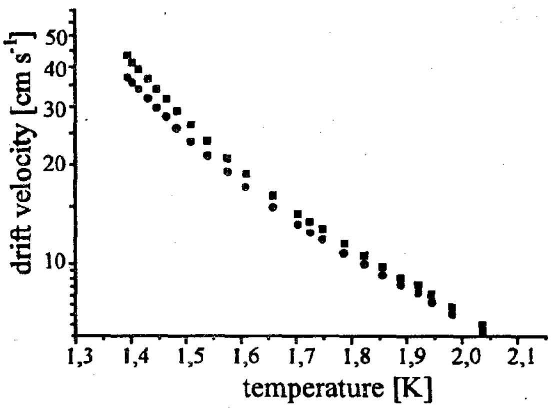

Fig. 5. The drift velocity of Au^+ and He^+ ions as a function of temperature. Most likely the dots are due to Au^+ and the squares, due to He^+ ions.

which was also detected in every run is not assigned so far.

For Ag^+ ions also a great number of various fast ions are recorded (Fig. 3). In optical emission spectra the vibrational bands of Ag_2 and Ag_3 were found [3,21]. The emission light caused by the monomers, dimers, and trimers of Ag was recorded as a function of time and showed qualitatively that the Ag ion is the fastest particle, followed by $(Ag_2)^+$ and $(Ag_3)^+$.

In Fig. 4 the drift velocity of Na^+ ions is plotted versus the electric drift field set with the grids, diaphragms, and collector (Fig. 1). The drift velocities at different electric fields are calculated from time-of-flight spectra (Fig. 2). The error bars are predominantly caused by the long opening time of the gate grids, by the uncertainties in the temperature measurement and, likely, by a field leakage into the drift area due to the high voltage at the sample. The statistic errors within a one-day run are estimated to be about one order of magnitude less important than the systematic errors.

In Fig. 5 the drift velocity of Au^+ and He^+ ions is plotted versus temperature. The data points show a slight deviation from an exponential temperature dependence for $T > 1.6$ K. This may be attributed to the fact that for a high roton density these elementary excitations can be no longer considered as dilute gas.

In addition to the mobility measurements with electrical detection of the ion current, an optical camera system was used. An image intensifying CCD

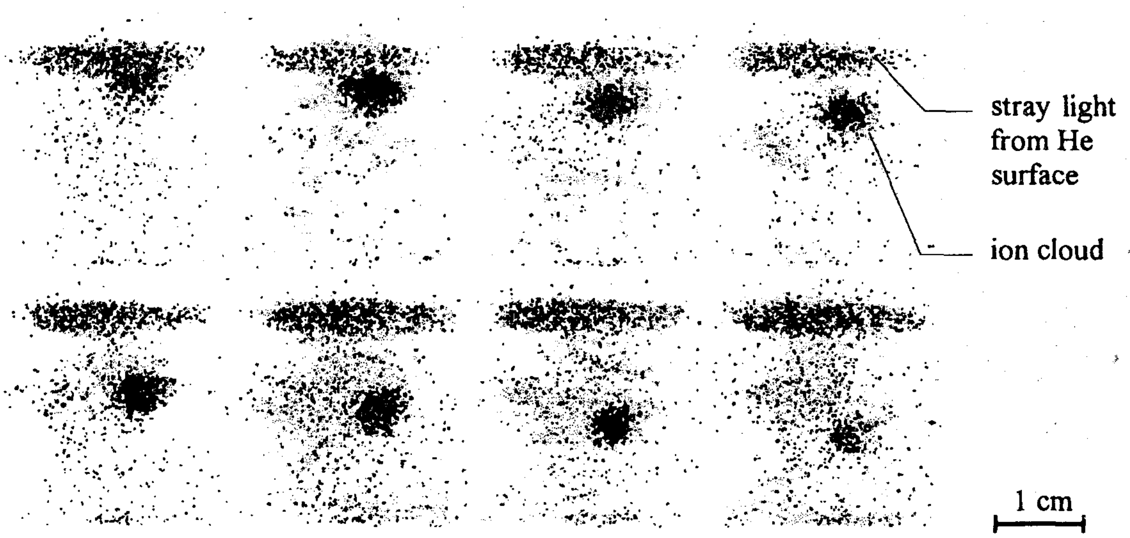

Fig. 6. CCD image of Ba^+ ions moving through liquid helium (top left to bottom right). The time interval between the upper four images is $100\ \mu s$, the interval between the lower images is $200\ \mu s$. High photon density is represented as darkening. Each ion cloud includes 10^5 to 10^6 photons.

device [22] served to visualize the motion of a cloud of Ba^+ ions in electric field (Fig. 6). During a short period of time (500 μs) a disc of Ba^+ ions is implanted into liquid helium to drift subsequently towards the negative electron emission tip (electric potential of −3 kV) [3,15]. The Ba^+ ions recombine one after another with electrons to form neutral atoms, producing the recombination light which is recorded by the camera. The measurement serves to monitor and to improve the electric drift field for optical emission and absorption studies [3,15] as well as to prepare optical studies of the dynamics of quantized vortices [23]. The counting of photons through the CCD device allowed us to estimate the number density of ions implanted by one single laser shot. Without any gated grids this number is estimated to be 10^8 to 10^9 ions and in the series of images (Fig. 6), 10^5 to 10^6. Thus, about 10^5 photons emitted into a steric angle of 4π are sufficient for temporal and spatial resolved studies.

4. Summary and outlook

In this contribution the low-field velocities of Na^+ and Au^+ ions as a function of temperature and electric drift field are presented. A variety of unexpected signals in the time-of-flight spectra are discovered which could be assigned only partially to single charged Na^+, Au^+, and He^+ ions. Some of the peaks can possibly be explained by molecular ions and impurities at the surface of the samples. In the case of Ag^+ ions so far no assignment to the observed peaks could be made. To clarify the situation, spectral studies on drifting ions are in preparation. Through laser induced fluorescence and recombination spectra it will be possible to distinguish between different moving charged particles.

The mobility measurements of foreign ions for the first time are extended to the λ-point providing additional data beyond the kinetic regime. In the temperature range above 1.7 K the ion–roton interaction must be considered in a special treatment. One crucial point in a better understanding of the roton–ion scattering process is the knowledge of the relevant effective masses. Here detailed studies of the defect structures as a function of temperature and pressure are necessary.

Acknowledgments

We are thankful to B. Tabbert for his continuous interest and support and for his help with implementing the CCD camera system. The authors acknowledge very fruitful discussions with L. P. Mezhov-Deglin. This work was sponsored by Deutsche Forschungsgemeinschaft.

1. L. Tisza, *Nature* **141**, 913 (1938).
2. H. Bauer, M. Hausmann, R. Mayer, H. J. Reyer, E. Weber, and A. Winnacker, *Phys. Lett.* **110A**, 279 (1985); H. Bauer, M. Beau, B. Friedl, C. Marchand, K. Miltner, and H. J. Reyher, *Phys. Lett.* **A146**, 134 (1990).
3. B. Tabbert, M. Beau, H. Günther, W. Häussler, C. Höninger, K. Meyer, B. Plagemann, and G. zu Putlitz, *Z. Phys.* **B97**, 425 (1995).
4. See the revelant contributions in: H. Günther, G. zu Putlitz, and B. Tabbert (eds.), *Proc. Symp. Ions and Atoms in He II (May 1994, Heidelberg), Z. Phys.* B98 (1995), p. 297-446.
5. K. R. Atkins, *Phys. Rev.* **116**, 1339 (1959).
6. M. W. Cole and R. A. Bachman, *Phys. Rev.* **B15**, 1388 (1977).
7. J. Poitrenaud and F. I. B. Williams, *Phys. Rev. Lett.* **29**, 1230 (1972); *Phys. Rev. Lett.* **32**, 1213 (1974).
8. D. G. Henshaw and A. D. B. Woods, *Phys. Rev.* **121**, 1266 (1961).
9. F. Reif and L. Meyer, *Phys. Rev.* **119**, 1164 (1960).
10. T. Ellis, P. V. E. McClintock, R. M. Bowley, and D. R. Allum, *Phil. Trans. Roy. Soc.* **296**, 581 (1980).
11. W. I. Glaberson and W. W. Johnson, *J. Low. Temp. Phys.* **20**, 313 (1975).
12. F. Reif and L. Meyer, *Phys. Rev.* **123**, 727 (1961).
13. R. M. Bowley, *J. Phys.* **C4**, 1645 (1971).
14. R. Barrera and G. Baym, *Phys. Rev.* **A6**, 1558 (1972).
15. H. Günther, M. Foerste, C. Honninger, G. zu Pulitz, and B. Tabbert, in: *Proc. Symp. Ions and Atoms in He II*, H. Günther, G. zu Putlitz, B. Tabbert (eds.), *Z. Phys.* **B98**, 395 (1995).
16. H. Bauer, M. Hausmann, R. Mayer, H.J. Reyher, E. Weber, and A. Winnacker, *Phys. Lett.* **A110A**, 279 (1985).
17. M. R. Beau, J. Fischer, G. zu Putlitz, and H. Schreck, *Proc. 14th Int. Conf. Coherent and Nonlinear Optics (ICONO'91)*, St. Petersburg, Russia (1991).
18. F. Pobell, *Matter and Methods at Low Temperatures*, Springer Verlag, Berlin — Heidelberg — New York (1992).
19. M. Beau, H. Günther, G. zu Putlitz, and B. Tabbert, *Z. Phys.* B99 (1996) (to be published).
20. H. Günther, M. Foerste, G. zu Putlitz, and T. Schumacher, *Z. Phys.* B (to be submitted).
21. M. R. Beau and G. zu Putlitz, *Proc. Symp. Atomic and Surface Physics (SASP 92)*, Pampeago/Tesreo-Trentino (1992).
22. B. Tabbert, M. Beau, M. Foerste, H. Günther, C. Hönninger, H. P. Hust, K. Layer, G. zu Putlitz, and T. Schumacher, in: *Proc. Symp. Ions and Atoms in He II*, H. Günther, G. zu Putlitz, B. Tabbert (eds.), *Z. Phys.* **B98**, 399 (1995).
23. H. Günther, F. Mayer, K. Meyer, B. Plagemann, G. zu Putlitz, and B. Tabbert, *Proc. 1st Int. Workshop Quantum Vorticity and Turbulence in He II Flows*, MPI Stromungsforschung Göttingen, Bericht 2/1994, G. Stamm, W. Fiszdon (eds.), Göttingen (1994).